Hydrogen Release from Dialkylamine–Boranes Promoted by Mg and Ca Complexes: A DFT Analysis of the Reaction Mechanism

3 AUTHORS:

Valeria Butera
Technion - Israel Institute of Technology
7 PUBLICATIONS **42** CITATIONS

SEE PROFILE

Nino Russo
Università della Calabria
512 PUBLICATIONS **7,941** CITATIONS

SEE PROFILE

Emilia Sicilia
Università della Calabria
151 PUBLICATIONS **1,942** CITATIONS

SEE PROFILE

▌Dehydrogenation

Hydrogen Release from Dialkylamine–Boranes Promoted by Mg and Ca Complexes: A DFT Analysis of the Reaction Mechanism

Valeria Butera,[a] Nino Russo,[a, b] and Emilia Sicilia*[a]

Abstract: Mg and Ca β-diketiminato silylamides [HC{(Me)CN(2,6-iPr$_2$C$_6$H$_3$)}$_2$M(THF)$_n${N(SiMe$_3$)$_2$}] (M = Mg, n = 0; M = Ca, n = 1) were studied as precatalysts for the dehydrogenation/dehydrocoupling of secondary amine–boranes R$_2$HNBH$_3$. By reaction with equimolar quantities of amine–boranes, the corresponding amidoborane derivatives are formed, which further react to yield dehydrogenation products such as the cyclic dimer [BH$_2$–NMe$_2$]$_2$. DFT was used here to explore the mechanistic alternatives proposed on the basis of the experimental findings for both Mg and Ca amidoboranes. The influence of the steric demand of amine–boranes on the course of the reaction was examined by performing calculations on the dehydrogenation of dimethylamine–borane (DMAB), pyrrolidine–borane (PB), and diisopropylamine–borane. In spite of the analogies in the cata-

lytic activity of Mg- and Ca-based complexes in the dehydrocoupling of amine–boranes, our theoretical analysis confirmed the experimentally observed lower reactivity of Ca complexes. Differences in catalytic activity of Mg- and Ca-based complexes were examined and rationalized. As a consequence of the increase in ionic radius on going from Mg^{2+} to Ca^{2+}, the dehydrogenation mechanism changes and formation of a key metal hydride intermediate becomes inaccessible. Dimerization is likely to occur off-metal in solution for DMAB and PB, whereas steric hindrance of iPr$_2$NHBH$_3$ hampers formation of the cyclic dimer. The reported results are of particular interest because, although amine–borane dehydrogenation is now well established, mechanistic insight is still lacking for many systems.

Introduction

The compound with the formal composition H$_3$NBH$_3$ has a long history.[1–6] First identified as a product of the reaction between ammonia and diborane, it can be prepared, depending on the conditions, in the form of the simple molecular adduct ammonia–borane, H$_3$NBH$_3$, and as a saltlike complex, the so-called diammoniate of diborane, [(H$_3$N)$_2$BH$_2$]$^+$[BH$_4$]$^-$. Ammonia–borane (AB) is a solid with sufficient stability at ambient temperatures for transport and storage. Replacing the hydrogen atoms of the ammonia fragment by alkyl substituents gives the alkylamine–boranes R$_n$H$_{3-n}$NBH$_3$, a series of molecular adducts which resemble ammonia–borane in being stable solids at ambient temperature. The coexistence of both hydridic B–H and protic N–H bonds in ammonia–borane and the alkylamine–boranes RH$_2$NBH$_3$ and R$_2$HNBH$_3$, in association

with a relatively strong coordinative B–N link, makes loss of dihydrogen more favorable than dissociation. Indeed, on heating or acid hydrolysis, these compounds release dihydrogen gas, but at a rate and with coproducts that depend markedly on the precise reaction conditions. Nevertheless, the combination of low molecular weight and high gravimetric hydrogen capacity (19.6 wt% for H$_3$NBH$_3$) has attracted intense interest in their use as media for chemical hydrogen storage,[7] as well as the potential reversibility of their dehydrogenation reactions.[8] To increase the rate of hydrogen release at a relatively low temperature, several strategies have been developed. In recent years, a series of new and in many cases improved catalysts for dehydrocoupling of AB and mono- and dialkylamine–boranes at room temperature based on a variety of early and late transition metals have been developed.[9] Comprehensive and detailed reviews are available on the chemistry of AB and amine–borane adducts and their potential as hydrogen-storage materials.[10] In this context, great interest has focused on the dehydrocoupling of secondary alkylamine–boranes in the hope that limiting the number of reactive protic N–H residues would provide less ambiguous intermediate species and systems which are more amenable to mechanistic study. Following this line of reasoning, we have previously studied catalysts based on Rh that can be used for the dehydrocoupling of secondary amine–boranes.[11] However, more recently, a considerable number of d^0 complexes of the cheaper and more abundant group 2 and group 13 metals in their highest oxidation states has been found to be effective in the dehydrogenation of

[a] Dr. V. Butera, Prof. N. Russo, Prof. Dr. E. Sicilia
Department of Chemistry
Università della Calabria
87036 Arcavacata di Rende (Italy)
Fax: (+39) 0984-492044
E-mail: siciliae@unical.it

[b] Prof. N. Russo
Departamento de Quimica, Division de Ciencias Basicas e Ingenieria
Universidad Autonoma Metropolitana-Iztapalapa
Av. San Rafael Atlixco No. 186, Col. Vicentina
CP 09340 Mexico, D.F. (Mexixo)

📄 Supporting information for this article is available on the WWW under http://dx.doi.org/10.1002/chem.201304329.

amine–boranes.[12] In contrast to the reactivity derived from low-oxidation-state or electron-richer catalytic centers, for such series of metals the possibility of B–H oxidative addition and/or B–N reductive elimination is excluded.

Hill and co-workers[12a–e] have carried out a broad survey of the catalytic activity of group 2 elements in dehydrocoupling reactions of amine–boranes and suggested that the process that leads to the formation of ultimate products, such as the cyclic dimer $[BH_2–NMe_2]_2$, is predominantly metal-mediated, in accordance with the mechanism illustrated in Scheme 1, which
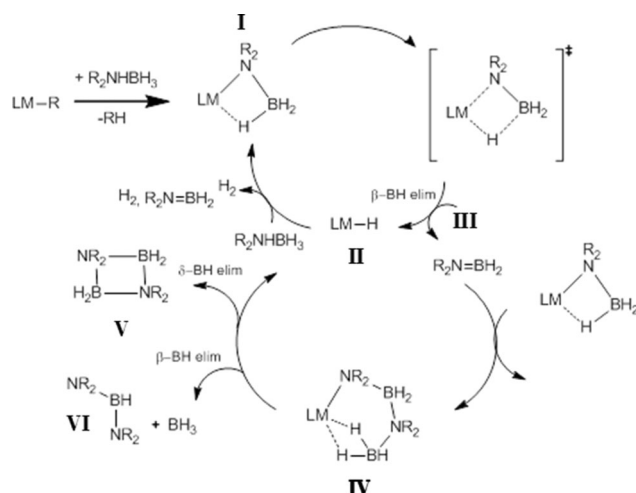
Scheme 1. Catalytic mechanism proposed for dehydrocoupling of amine–boranes.

accounts for the observed reactivity. The proposed mechanism is supported by the detection of the unsaturated species $BH_2=NR_2$ during the course of the reaction and the formation of the $[H_3BNR_2BH_2R_2N]^-$ anion alongside apparent metal-hydride formation. Catalytic B–N bond formation and turnover depend on production and insertion of the unsaturated species $R_2N=BH_2$ to yield a key catalytic intermediate containing the $[H_3BNR_2BH_2R_2N]^-$ ion. Subsequent formation of the amidoborane products $[H_2BNMe_2]_2$ and $HB(NR_2)_2$ is then dictated by the relative energetics of a sequence of steps consisting of β-hydride elimination from the metalated amidoborane, insertion of the polarized aminoborane, and δ-hydride elimination, eventually in competition with further β-hydride elimination. What emerges from these studies is that an increase in the charge density of the cation, as well as a decrease in the radius, results in an increase in dehydrocoupling activity and the ability of the cationic center to mediate each step involved in the catalytic cycle. Since the initial studies were concerned primarily with dimethylamine–borane (DMAB), the same authors extended their studies to a wider range of alkylamine–boranes and demonstrated that the proposed mechanism is not restricted to DMAB alone.[12c]

Density functional theory (DFT) was used herein to explore the mechanistic routes of the dehydrocoupling reaction of several more or less bulky amine–boranes according to the catalytic mechanism in Scheme 1. Given that the first step of the

process is likely to be formation of amidoborane derivatives as the true catalysts for amine–borane dehydrocoupling, the true mechanistic investigation starts from such species, which are formed by loss of an RH unit due to hydrogen-atom transfer from the entering amine–borane to the R group of the metal complex. In the present theoretical study, amidoborane complexes **I** are Mg and Ca β-diketiminato amidoborane derivatives of the form $[HC\{(Me)CN(2,6-iPr_2C_6H_3)\}_2MNR_2·BH_3$ (M = Mg, $n = 0$; M = Ca, $n = 1$), which are produced by reaction of the corresponding silylamides $[HC\{(Me)CN(2,6-iPr_2C_6H_3)\}_2M(THF)_n\{N-(SiMe_3)_2\}]$ with an equimolar quantity of amine–boranes R_2HNBH_3.[12b,c] Further reaction of the amine–boranes with such derivatives results in formation of species that are key intermediates in the proposed catalytic cycle in Scheme 1.

Once the metal amidoborane species **I** is formed, it can undergo a β-hydride elimination to form metal hydride LM–H (**II**) together with unsaturated aminoborane $R_2N=BH_2$ (**III**). At this point the reaction pathway bifurcates. On the one hand, metal hydride species **II** can react directly with another amine–borane molecule with loss of molecular hydrogen and regeneration of the starting amidoborane compound **I**. Alternatively, insertion of unsaturated species **III** into the M–N bond of metal hydride **II** could occur to give the anion $[H_3BNR_2BH_2R_2N]^-$ coordinated to the metal center (**IV**) Owing to the demonstrated olefin-like reactivity of aminoboranes,[13] it was hypothesized that the key B–N bond-forming step is the insertion of the olefin-isoelectronic aminoborane $R_2N=BH_2$ into the M–N bond. The resulting intermediate can be converted to the cyclic product $[R_2N–BH_2]_2$ (**V**) by a δ-hydride elimination. Alternatively, as a result of a further β-hydride elimination step minor quantities of diaminoboranes $HB(NR_2)_2$ (**VI**) are formed. The metal hydride **II** that is formed is poised to react with an additional amine–borane molecule to restore the amidoborane complex **I** and restart the catalytic cycle.

To date, it is still a difficult challenge to obtain experimentally direct and accurate insight into the mechanistic pathways of chemical reactions. The most important limitation is the fact that key intermediates often have a very short lifetime. This limitation holds also for the metal-catalyzed dehydrocoupling reactions of amine–boranes, such as those under examination in the present work; these are now well established, but their mechanisms are often unclear. Computational studies do not suffer from these limitations and therefore provide a valuable complementary approach to studying these reactions. The present study attempts to shed light on the underlying mechanism of the dehydrocoupling process, knowledge of which is indispensable for improvement of the reaction conditions and the application of such chemistry to a broader array of catalytic reactions.
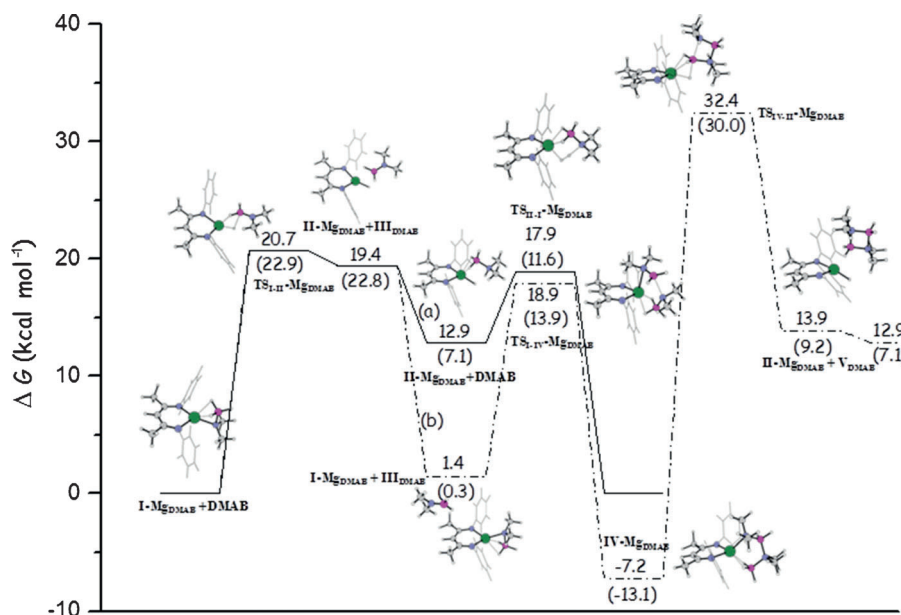
Results and Discussion

The DFT investigation was performed with a twofold purpose: to assess the viability of the pathways of the mechanistic scheme proposed by Hill and co-workers[12b–e] and to compare the behaviors of Mg and Ca complexes to determine whether differences in ionic radius and charge density can be consid-

⤪⤪ These are not the final page numbers!

ered to be responsible for the observed differences in reactivity. The influence of the steric demand of amine–boranes on the course of the reaction was examined by performing calculations on the dehydrogenation of dimethylamine–borane, (DMAB), pyrrolidine–borane (PB), and diisopropylamine–borane. To reduce the computational expense the β-diketiminato ligand was simplified by replacing the two *i*Pr substituents of the *N*-aryl groups with H atoms. Unless otherwise noted, the discussed energies are relative free energies calculated in THF solvent with respect to amidoborane complex **I**.

Figure 1. Calculated B3PW91 free energy profiles for the dehydrocoupling reaction of DMAB assisted by the amidoborane complex **I-Mg$_{DMAB}$**. Along pathway a (solid line) the formed hydride complex reacts with a second DMAB molecule, and along pathway b (dot-dashed line) the released aminoborane molecule inserts into the Mg—N bond of unreacted amidoborane. Gas-phase zero-point-corrected energy changes are reported in parentheses. Energies [kcal mol^{-1}] are relative to the asymptote of the reactants.
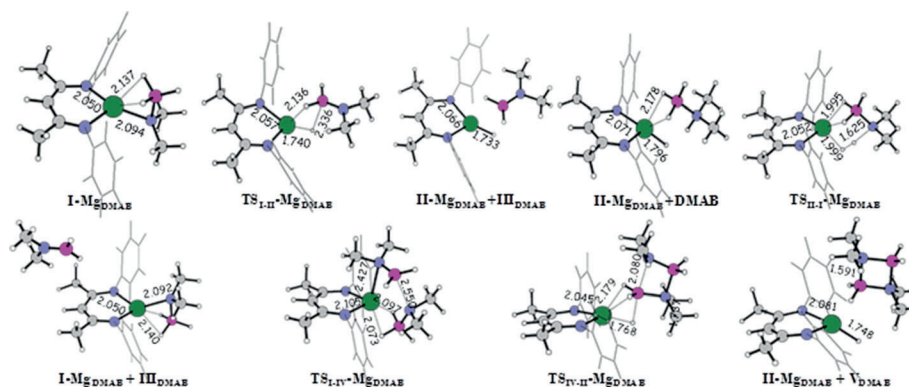
Mechanism of hydrogen release from DMAB promoted by the Mg amidoborane complex

The calculated B3PW91 free-energy profiles for the reaction between the Mg complex HC{(Me)CN(2,6-C$_6$H$_5$)}$_2$MgNMe$_2$·BH$_3$ (**I-Mg$_{DMAB}$**) and a DMAB molecule is shown in Figure 1. Figure 2 shows the structure of the intercepted stationary points, except that of the complex containing the anion coordinated to the metal center, which is depicted in Figure 3. The Supporting Information gives the geometries of all the optimized structures shown here.

The amidoborane complex **I-Mg$_{DMAB}$** contains a pseudo-four-coordinate magnesium center

Figure 2. Fully optimized DFT structures of stationary points intercepted along DMAB dehydrocoupling pathways a and b assisted by the β-diketiminato Mg amidoborane complex **I-Mg$_{DMAB}$**. Selected bond lengths are provided in angstroms.

with the coordination sphere provided by the bidentate β-diketiminato ligand and the chelating anion of the DMAB molecule interacting with magnesium through the formally deprotonated nitrogen atom and BH groups from the BH$_3$ component of DMAB. Transfer of an H atom from the B atom to the Mg center occurs by overcoming a free-energy barrier of 20.7 kcal mol^{-1}, corresponding to the **TS$_{I-II}$-Mg$_{DMAB}$** transition state for BH/MgN σ-bond metathesis. The normal mode associated with a calculated imaginary frequency of 140i cm^{-1} corresponds to stretching of the B—H bond, which allows transfer of the H atom to Mg. Boron hybridization changes from sp^3 to sp^2, whereas the nitrogen atom appears to remain detached. The formed products, that is, the magnesium hydride **II-**

Mg$_{DMAB}$, and the aminoborane Me$_2$N=BH$_2$ (**III$_{DMAB}$**) are only 1.3 kcal mol^{-1} more stable than the preceding transition state. As illustrated in Figure 1, the next step, along pathway a, can be the reaction of the hydride **II-Mg$_{DMAB}$** with a second molecule of DMAB to release molecular hydrogen and regenerate the **I-Mg** complex, which is poised to restart the catalytic cycle. Alternatively, on pathway b the generated aminoborane **III$_{DMAB}$** can insert into the Mg—N bond of the unreacted amidoborane **I-Mg$_{DMAB}$** to form what is considered to be a key catalytic intermediate, that is, complex **IV-Mg$_{DMAB}$** containing the [H$_3$BNR$_2$BH$_2$R$_2$N]$^-$ anion.

Interaction of the Mg hydride with a second DMAB molecule (pathway a) results in a stabilization of 12.9 kcal mol^{-1}. From

These are not the final page numbers! ↗↗
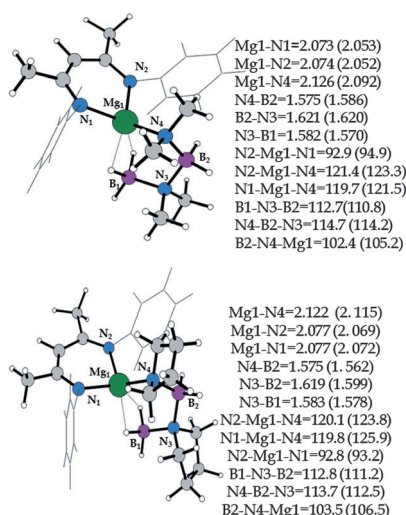
Figure 3. DFT optimized geometrical structure of β-diketiminato Mg complexes with the $[H_3BNMe_2BH_2Me_2N]^-$ and $[H_3BN(CH_2)_4BH_2(CH_2)_4N]^-$ anions coordinated to the metal center. Selected bond lengths [Å] and angles [°] are compared with available experimental values (in parentheses).

the formed adduct **II-Mg$_{DMAB}$+DMAB** molecular hydrogen loss occurs via **TS$_{II-I}$-Mg$_{DMAB}$** with a low free-energy barrier of 5.3 kcal mol^{-1}. The intercepted transition state is characterized by an imaginary frequency of $210i$ cm^{-1} and the associated normal mode mainly corresponds to the stretching of the Mg—H and N—H bonds. As a result, the initial complex **I-Mg$_{DMAB}$** is regenerated and by reaction with a new DMAB molecule the catalytic cycle can restart.

Along the pathway b, the released unsaturated aminoborane R$_2$N=BH$_2$ instead reacts with unreacted amidoborane complex **I-Mg$_{DMAB}$** to afford the **IV-Mg$_{DMAB}$** complex. The free-energy barrier of transition state **TS$_{I-IV}$** for this transformation is 16.5 kcal mol^{-1}. The structure of the transition state and the calculated imaginary frequency reveal that the aminoborane coordinates to the Mg center through the nitrogen atom and inserts into the Mg—N bond of amido complex **I-Mg$_{DMAB}$**. The formed **IV-Mg$_{DMAB}$** complex, which in solution lies 1.8 kcal mol^{-1} above the entrance channel of the reaction, contains a pseudo-four-coordinate magnesium center, the coordination sphere of which is provided by the bidentate β-diketiminato ligand and the chelating $[H_3BNMe_2BH_2Me_2N]^-$ ion. The anion interacts with the Mg center primarily through the formally deprotonated nitrogen atom and the B—H groups of the BH$_3$ unit. Such a compound has been characterized by single-crystal X-ray diffraction. A comparison of the calculated and experimental values of the most relevant geometrical parameters is given in Figure 3. The very good agreement between theoretical and experimental values proves the reliability of the reported results and the suitability of the employed computational protocol. A BH hydride δ-elimination leads from intermediate **IV-Mg$_{DMAB}$** to the elimination of the cyclic dimer [Me$_2$N—BH$_2$]$_2$ (**V$_{DMAB}$**) and restoration of the **II-Mg$_{DMAB}$** intermediate. Nevertheless, for this elimination to occur it is necessary to surmount a high free-energy barrier of 39.6 kcal mol^{-1} for the transition state **TS$_{IV-II}$-Mg$_{DMAB}$**. The imaginary frequency of $628i$ cm^{-1},

which confirms the nature of transition state of the intercepted stationary point, corresponds to the transfer of a BH hydride to the Mg center together with the formation of a new B—N bond. The reaction of the regenerated magnesium hydride complex with an additional amine–borane molecule, in accordance with the description of the mechanistic steps along pathway a, yields again the initial Mg amidoborane complex.

For the sake of completeness, the mechanism of the reaction that, as a result of a further, eventually competitive, β-hydride elimination step from the **IV-Mg$_{DMAB}$** intermediate, can afford the observed diaminoborane species HB(NMe$_2$)$_2$ by loss of a BH$_3$ unit was also examined. The structures of the intercepted intermediates and transition states and their energetics are provided in Figure S2 of the Supporting Information. Our calculations clearly show that this pathway is not viable. The process is not concerted, and should occur in two steps. In the first step, the β-hydride is transferred to the terminal BH$_3$ group to form a BH$_4^-$ anion that coordinates to the metal center and the formed aminoborane is simultaneously eliminated. In a second step an H atom from the anion is transferred to metal atom to restore the **II-Mg$_{DMAB}$** intermediate. The calculated barrier for the β-BH transfer of 55.3 kcal mol^{-1} is very high. The situation is even worse for formation of the final products (**II-Mg$_{DMAB}$** + BH$_3$ + HB(NMe$_2$)$_2$), which are calculated to be completely inaccessible, as they lie 57.1 kcal mol^{-1} above the reference energy of the **IV-Mg$_{DMAB}$** intermediate. This reaction channel is disregarded in the calculations reported below.

Our theoretical exploration of the mechanism proposed to account for the experimental observations shows that the pathway on which reaction of the generated Mg hydride complex with an additional DMAB molecule leads to elimination of an H$_2$ molecule and regeneration of the **I-Mg$_{DMAB}$** catalyst is the most favorable. Along the pathway that involves formation of the complex containing the anion $[H_3BNR_2BH_2R_2N]^-$ coordinated to the metal center, the rate-determining step is the elimination of the cyclic dimer **V$_{DMAB}$**. The high energy barrier that hampers the formation of **V$_{DMAB}$** makes pathway b impracticable, or, at least, it is unlikely that, once intermediate **IV-Mg$_{DMAB}$** is formed, the reaction can proceed to form the final product. Intermediate **IV-Mg$_{DMAB}$** sits in a deep well and for that reason should be detectable and characterizable. The barrier of 39.6 kcal mol^{-1} for the formation of the next minimum can be compared with the barrier calculated for off-metal uncatalyzed dimerization.[11] The calculations show that off-metal dimerization is exothermic (4.2 kcal mol^{-1}), as it should be,[9h] and has a free-energy barrier of 20.5 kcal mol^{-1}, which is in good agreement with that experimentally determined of 18.2 ± 2.9 kcal mol^{-1}.[14] As a consequence, free monomers, once released, should form the cyclic dimer [Me$_2$N—BH$_2$]$_2$ in solution without involvement of the Mg complex. The possibility was taken into consideration that such independently formed cyclic dimers can react with the magnesium hydride species **I-Mg$_{DMAB}$** to produce the **IV-Mg$_{DMAB}$** complex. In the energy profile shown in Figure 1, from the right- to the left-hand side, a calculated energetic cost of such a transformation of about 18 kcal mol^{-1} results, which is comparable to the energy barrier

🡤🡤 **These are not the final page numbers!**

of 16.5 kcal mol^{-1} for the formation of the **IV-Mg$_{DMAB}$** complex by insertion of the aminoborane $R_2N{=}BH_2$ into the Mg–N bond of the amidoborane **I-Mg$_{DMAB}$** catalyst. However, an experiment carried out to prove whether the products of δ-hydride elimination could combine to form the anion observed in **IV-Mg$_{DMAB}$** did not give any corroboration of this hypothesis.

Dehydrocoupling of alkylamine–boranes promoted by the Mg β-diketiminato complex

To determine the influence of the substrate on the energetics of the process, mainly due to the steric hindrance of alkyl substituents, analogous calculations were carried out for Mg β-diketiminato amidoborane derivatives of PB and diisopropylamine–borane. Reaction pathways a and b were both examined, and the corresponding results are summarized in Figures 4 and 5, respectively. Fully optimized geometrical structures of stationary points and Cartesian coordinates are given in the Supporting Information.

The dehydrocoupling reaction of the Mg β-diketiminato pyrrolidine–borane amidoborane derivative has been experimentally examined,[12c] whereas for diisopropylamine–borane experimental information on the same process was obtained by considering the magnesium amidoborane species formed by reaction with the homoleptic silylamide [Mg{N(SiMe$_3$)$_2$}$_2$]. In the former case, different products were observed as a function of the reaction stoichiometry. In presence of one equivalent of PB, complete consumption of the substrate leads to formation of an apparent amidoborane complex, whereas with two equivalents of PB the formation of the complex containing the anion [H$_3$BN(CH$_2$)$_4$BH$_2$(CH$_2$)$_4$N]$^-$ was detected, which is indicative of a behavior analogous to that of DMAB magnesium amidoborane. On the contrary, when the more sterically demanding iPr$_2$NHBH$_3$ reacts with the magnesium silylamide [Mg{N(SiMe$_3$)$_2$}$_2$], the only observed product is iPr$_2$N{=}BH$_2$, whereas no
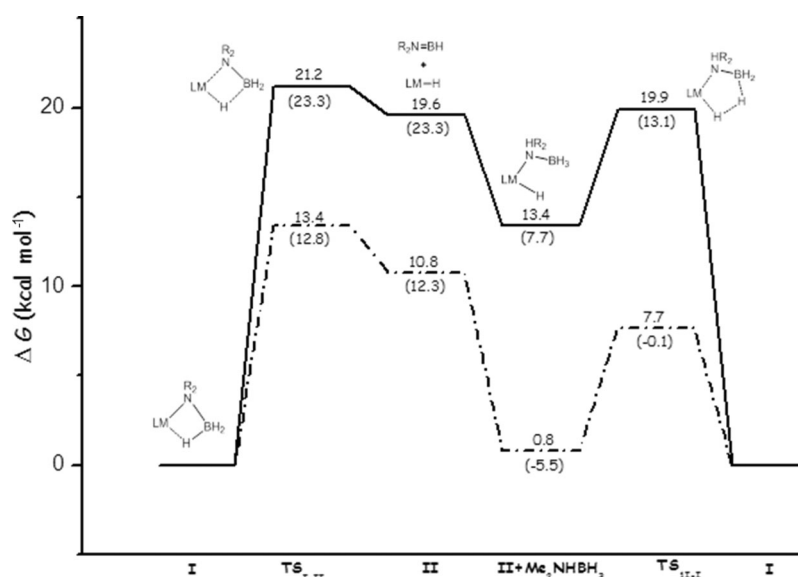
Figure 4. Calculated B3PW91 free-energy profiles for the dehydrocoupling of PB (solid line) and iPr$_2$NHBH$_3$ (dot-dashed line) assisted by the corresponding Mg amidoborane complexes along pathway a. Gas-phase zero-point-corrected energy changes are reported in parentheses. Energies [kcal mol^{-1}] are relative to the asymptote of the reactants.
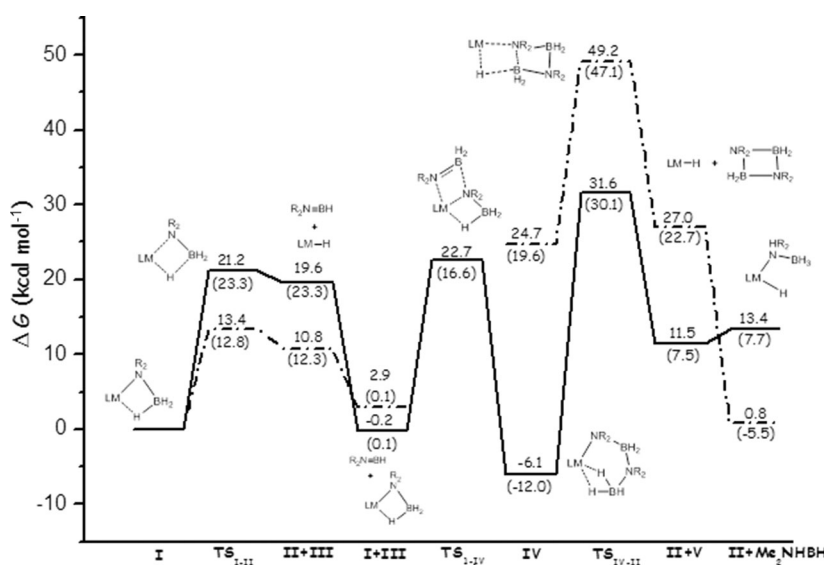
Figure 5. Calculated B3PW91 free-energy profiles for the dehydrocoupling of PB(solid line) and iPr$_2$NHBH$_3$ (dot-dashed line) assisted by the corresponding Mg amidoborane complexes along pathway b. Gas-phase zero-point-corrected energy changes are reported in parentheses. Energies [kcal mol^{-1}] are relative to the asymptote of the reactants.

evidence for formation of the [H$_3$BNiPr$_2$BH$_2$$iPr_2$N]$^-$ anion exists. The outcome of our theoretical exploration is in agreement with the experimental findings and is helpful in their rationalization. As illustrated in Figures 4 and 5 the first common step of both pathways a and b, that is, the BH/MgN σ-bond metathesis that leads to the formation of the β-diketiminato Mg hydride species, occurs by overcoming an energy barrier of 21.2 and 13.4 kcal mol^{-1} for the **TS$_{I-II}$** transition state of PB and iPr$_2$NHBH$_3$, respectively. The height of the activation-energy

These are not the final page numbers! ↗↗

barrier calculated for PB is comparable to that of DMAB, whereas the barrier for the β-hydride elimination from iPr$_2$NHBH$_3$ is about 7 kcal mol^{-1} lower. This difference in behavior can be ascribed to the presence of the more electron donating iPr groups on nitrogen. Indeed, as is expected and confirmed by the NBO population analysis, the charge-density distribution (Figure S5 of the Supporting Information) is more favorable for the β-BH hydride release. Further support comes from the calculated values of the bond length between the boron atom and the H atom that is transferred to the Mg center, which is 1.244 Å for DMAB and PB and 1.255 Å for iPr$_2$NHBH$_3$. The eliminated aminoborane **III** and the formed magnesium hydride **II** are only about 2 kcal mol^{-1} more stable than the preceding transition state in both cases. Interaction of complex **II** with a second amine–borane molecule causes a stabilization of 6.2 kcal mol^{-1} for PB and 10.0 kcal mol^{-1} for iPr$_2$NH·BH$_3$.

From the adduct between intermediate **II** and an additional amine–borane, an H$_2$ molecule is eliminated and the starting amidoborane complex is regenerated via the **TS$_{II-I}$** transition state with a barrier of about 7 kcal mol^{-1} for both PB and iPr$_2$NHBH$_3$ substrates. Alternatively, along pathway b, the eliminated aminoborane **III** can react with the amidoborane catalyst **I** to form complex **IV**, which contains the anion formed by insertion of the aminoborane **III** into the Mg—N bond of the amidoborane complex. The fully optimized structure of complex **IV** formed by reaction with PB is shown in Figure 3, in which calculated and experimental values of selected geometrical parameters are also reported. The barrier for the transition state **TS$_{I-IV}$** was calculated to be 19.8 kcal mol^{-1} for PB. However, all attempts to locate an analogous transition state for this transformation of iPr$_2$NHBH$_3$ were unsuccessful, most likely because of the greater steric demand of the involved aminoborane, which hinders insertion into the Mg—N bond of the amidoborane. The formed intermediate **IV** along the dehydrocoupling pathway of PB is stabilized by 6.1 kcal mol^{-1} with respect to the entrance channel, whereas for iPr$_2$NHBH$_3$ an endothermicity of 24.7 kcal mol^{-1} was calculated. Finally, to release the cyclic dimer and restore the corresponding Mg hydride it is required to overcome a barrier of 37.7 and 24.5 kcal mol^{-1} for PB and iPr$_2$NHBH$_3$, respectively. In analogy with DMAB, the feasibility of self-dimerization for the PB and iPr$_2$NHBH$_3$ substrates in solution was also examined. The calculated pathways are shown in Figure S6 of the Supporting Information. The (CH$_2$)$_4$N≡BH$_2$ monomers can undergo off-metal dimerization by overcoming an energy barrier of 24.4 kcal mol^{-1} and the reaction is thermoneutral. The aminoborane iPr$_2$N≡BH$_2$ was experimentally demonstrated to be resistant to self-dimerization.[15] Calculations confirm that the energy barrier that must be surmounted is very high (40.3 kcal mol^{-1}), and the cyclic dimer that would be produced lies 20.1 kcal mol^{-1} above the dissociation limit of the reactants. In summary, for diisopropylamine–borane the only viable path is that involving release of the iPr$_2$N≡BH$_2$ monomer and activation of a second amine–borane molecule assisted by the Mg hydride intermediate, formation of which is favored by the electron-donating nature of the iPr groups. Alternative reactions as well as self-dimerization are precluded by the steric hindrance of the same alkyl groups. For the less sterically demanding PB substrate, although formation of the magnesium hydride and loss of the corresponding aminoborane molecule is less facile, the subsequent reaction with an additional substrate molecule is straightforward, and the reaction with the unreacted amidoborane to yield the intermediate containing the [H$_3$BN(CH$_2$)$_4$BH$_2$(CH$_2$)$_4$N]$^-$ anion is not precluded. Our calculations do not support the hypothesis that the cyclic dimer could be released from the accessible intermediate **IV**. The height of the barriers for the dimerization of the aminoborane monomers and for the reaction of the magnesium hydride with the released (CH$_2$)$_4$N≡BH$_2$ monomer to form intermediate **IV** are calculated to be 24.4 and 19.8 kcal mol^{-1}, respectively. According to experiments, for iPr$_2$NHBH$_3$ neither the [H$_3$BNiPr$_2$BH$_2$(CH$_2$)$_4$N]$^-$ anion nor the cyclic dimer [iPr$_2$N-BH$_2$]$_2$ can be formed.

Mechanism of hydrogen release from dialkylamine–boranes promoted by Ca amidoborane complexes

Calcium-based complexes, although less reactive than their magnesium counterparts, show similar reactivity in dehydrocoupling reactions and yield similar products when thermally promoted catalytic conditions are employed.[12b,c] For that reason the general reactivity pattern shown in Scheme 1, assumed to describe the viable pathways for all group 2 metal complexes, should also be valid for amine–borane dehydrocoupling reactions assisted by Ca catalysts. Experiments on the Ca β-diketiminato silylamide [HC{(Me)CN(2,6-iPr$_2$C$_6$H$_3$)}$_2$Ca-(THF){N(SiMe$_3$)$_2$}] and DMAB clearly evidenced formation of the corresponding amidoborane [HC{(Me)CN(2,6-iPr$_2$C$_6$H$_3$)}$_2$CaNMe$_2$·BH$_3$.[12b] Further reactivity of the detected amidoborane was suggested on the basis of NMR spectra and their similarities with analogous spectra recorded during the dehydrocoupling reaction of DMAB assisted by Mg amidoboranes. Although NMR spectra support only the formation of monomeric Me$_2$N≡BH$_2$, the authors do not totally exclude that β-diketiminato calcium hydride and dimeric [Me$_2$N—BH$_2$]$_2$ species could be formed. The reduced facility of β-hydride elimination and B—N coupling for group 2 elements heavier than magnesium has been confirmed by these results. Analogous conclusions have been drawn on the basis of the experimental findings for the reaction of [HC{(Me)CN(2,6-iPr$_2$C$_6$H$_3$)}$_2$Ca-(THF){N(SiMe$_3$)$_2$}] with PB and [Ca{N(SiMe$_3$)$_2$}$_2$] with iPr$_2$NHBH$_3$. Overall, experiments support only formation of the corresponding Ca amidoborane complexes and, under appropriate conditions, of the aminoboranes. In particular, for iPr$_2$NHBH$_3$, clean and selective conversion to iPr$_2$N≡BH$_2$ on addition of two equivalents of the amine–borane was assumed to indicate that that dehydrogenation should be assisted by coordination of a further molecule of iPr$_2$NHBH$_3$. The fully optimized structures of the Ca amidoborane complexes formed by reaction with DMAB and PB substrates are shown in Figure 6, which also compares the calculated and experimental values of selected bond lengths and angles. The reproduction of the experimental geometrical parameters of the complex is good. The Ca center is coordinated by the β-diketiminato ligand, the dime-
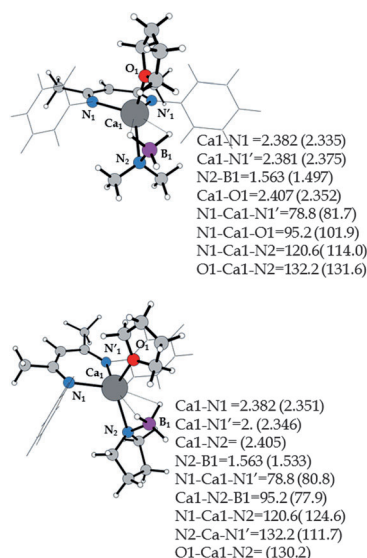
Figure 6. DFT optimized geometrical structure of β-diketiminato Ca amidoboranes of DMAB and PB. Selected bond lengths [Å] and angles [°] are compared with available experimental values (in parentheses).

thylamidoborane through the formally deprotonated nitrogen atom and B–H groups of the BH$_3$ unit, and a THF solvent molecule.

At the beginning of our theoretical investigation, driven by the hypothesis that a calcium hydride should be formed, we used all suitable computational strategies to intercept the transition state that through BH β-elimination from the amidoborane **I** leads to release of the aminoborane R$_2$N=BH$_2$ with concomitant formation of calcium hydride **II**. All attempts to theoretically model the pathway that leads to the calcium hydride intermediate were unsuccessful. Moreover, the optimized structures of the β-diketiminato Ca hydrides are calculated to be less stable. For example, the Ca–H compound lies about 35 kcal mol^{-1} above the reference energy of the Ca DMAB amidoborane derivative. Therefore, all efforts were concentrated on the search for a viable alternative pathway. The energy profiles for the only pathway that appears to be practicable are shown in Figure 7, which also shows the structures of the intercepted stationary points for the reaction of the DMAB substrate. Cartesian coordinates are given in the Supporting Information along with the structures and Cartesian

coordinates of the analogous stationary points for PB and iPr$_2$NHBH$_3$.

In accordance with the previously drawn conclusion that the catalytic activity of calcium and magnesium β-diketiminato complexes is inhibited by Lewis bases such as THF as well as binding of substrate or product to the metal center,[16] only when the THF-free calcium catalyst **I-Ca$_{DMAB}$** is coordinated by a second DMAB molecule can a reaction take place. Intermolecular elimination of molecular hydrogen occurs by interaction of the NH proton of the aminoborane molecule and a BH hydride of the ligated amidoborane via transition state **TS1-Ca$_{DMAB}$** with a solvent-corrected free-energy barrier of 30.1 kcal mol^{-1}. As a consequence, the aminoborane Me$_2$N=BH$_2$ is also eliminated and the THF-free amidoborane catalyst is regenerated. Coordination of a further DMAB molecule restarts the catalytic cycle. The reaction proceeds in a very similar way for the other two examined substrates, and an energy barrier with the same height of 30.2 kcal mol^{-1} must be overcome when the involved aminoborane is PB. A change in behavior, in agreement with experimental evidence, occurs when the substrate is iPr$_2$NHBH$_3$. Both the steric hindrance and the electron-donating nature of the iPr groups cooperate in lowering the height of the activation barrier, which is calculated to be 22.7 kcal mol^{-1}. The charge induction enhances the charge polarization of the BH hydride and the acidity of the NH proton. The steric hindrance of the iPr groups on the nitrogen atom of the amidoborane causes an elongation of the Ca–N bond favoring the release of iPr$_2$N=BH$_2$. The difference in height of the activation barriers allows rationalization of the experimental findings. Once the amidoborane complex is formed, in all cases further addition of a second amine–borane molecule is required for the dehydrogenation reaction to proceed. However, for DMAB
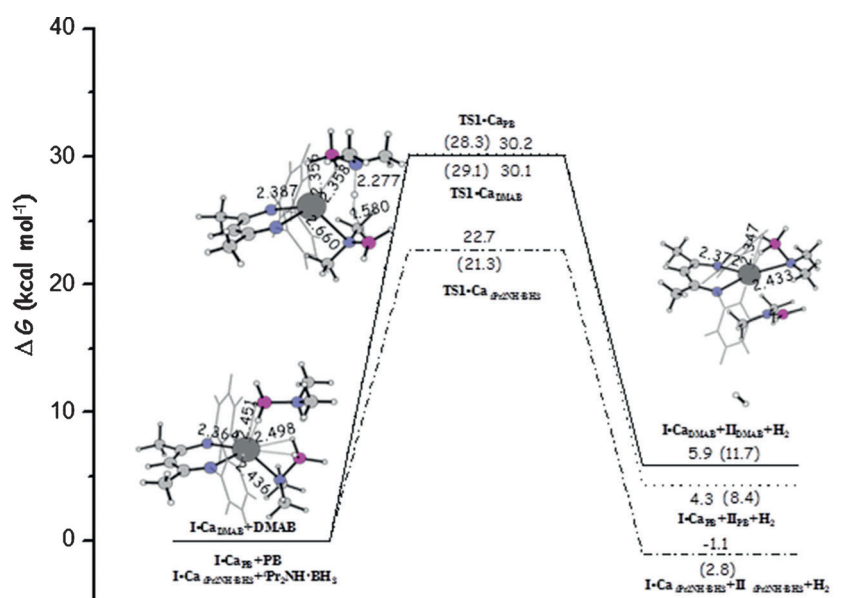
Figure 7. Calculated B3PW91 free-energy profiles for the dehydrogenation of DMAB (solid line), PB (dashed line), and iPr$_2$NHBH$_3$ (dot-dashed line) promoted by the corresponding β-diketiminato Ca amidoboranes. Gas-phase zero-point-corrected energy changes are reported in parentheses. Energies [kcal mol^{-1}] are relative to the asymptote of the reactants.

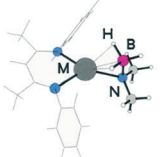**These are not the final page numbers!** ↗↗

and PB substrates, due to the barriers which hamper product formation, only by heating the sample can the corresponding aminoboranes be formed and detected.

Effects of cation charge density and radius

Our theoretical investigation clearly demonstrated that, in spite of the apparent analogy in behavior of the examined Mg- and Ca-based catalyst systems toward amine–borane dehydrocoupling, overgeneralizations, as recommended by Hill and co-workers,[12c] must be avoided. The observed difference in catalytic activity of Mg- and Ca-based catalysts systems has been assumed to depend on the decreased stability of formed amidoboranes toward β-hydride elimination on going from Mg to Ca. According to Scheme 1, the products of such β-H elimination should be the corresponding metal hydride and an aminoborane molecule, both poised to react further. Our calculations show that, when the metal is Ca, only after precoordination of an additional amine–borane molecule to the metal center can β-H elimination occur to release molecular hydrogen, whereas formation of a Ca hydride intermediate is not feasible. Hence, the reaction mechanism changes. The transfer of an H atom to the Ca center does not occur, and the increase in the ionic radius and the resultant charge density at the metal center should be at the origin of this behavior. The results of NBO charge analysis and the most relevant bond lengths are compared in Table 1. For Ca the calculated values

Table 1. Selected NBO charges and bond lengths of Mg and Ca β-diketiminato amidoborane derivatives.

	NBO charge		Bond length [Å]		
	H	M	M–H	M–N	M–B
I-Ca$_{DMAB}$, THF-free	−0.084	1.622	2.354	2.384	2.510
I-Ca$_{DMAB}$, THF-solvated	−0.079	1.540	2.406	2.408	2.560
I-Mg$_{DMAB}$	−0.051	1.483	2.137	2.094	2.241

of both THF-free and THF-solvated complexes are listed. The Ca cation bears a positive charge (+1.622 and +1.540, respectively) greater than that on Mg (+1.483). Since the BH hydrogen atom that is transferred carries a partial negative charge, a shift to the calcium center should be more favorable. Nevertheless, as a consequence of the increase in ionic radius from 0.72 Å for Mg^{II} to 1.00 Å for Ca^{II} (in six-coordinate complexes), the bond lengths between the metal center and the nitrogen and boron atoms of the coordinated amidoborane are considerably longer for Ca than Mg. It can be proposed that, because the distance between the Ca center and the BH hydride is too long, transfer cannot occur.

The Ca hydride complex that would be formed by β-hydride transfer, as described above, is significantly less stable than the corresponding amidoborane complex, whereas formation of

the Mg hydride complex is almost thermoneutral (see Figure 1). The calculated Mg–H bond length of 1.734 Å compares well with the experimentally estimated values, which range from 1.72(3) to 1.90(3) Å, depending the environment.[12j] The calculated Ca–H bond length of 2.057 Å is significantly longer and in line with the hypothesis that the bonding interaction, at least in monometallic species, is too weak to provide access to formation of the hydride complex.

Conclusion

To establish whether inexpensive group 2 complexes can function as catalysts for the dehydrocoupling of amine–borane substrates equally well as electron-rich middle and late transition metal species, a detailed theoretical exploration of the mechanistic scenario put forward on the basis of experimental evidence was carried out. Catalytic activity of β-diketiminato Mg and Ca silylamides toward dehydrocoupling of dimethylamine–borane, pyrrolidine–borane, and diisopropylamine–borane substrates was examined. The differences in catalytic activity of Mg and Ca complexes were rationalized, as well as the influence of the steric hindrance of the alkyl substituents on nitrogen on the mechanism. The formed Mg amidoboranes undergo BH/MgN σ-bond metathesis to form the corresponding hydrides. The reaction pathway then bifurcates. The hydride complex can react along pathway a with a second amine–borane molecule to eliminate molecular hydrogen and restore the amidoborane catalyst. Alternatively, along a pathway b the released aminoborane molecule can insert into the Mg–N bond of the unreacted amidoborane to form a complex containing the [H$_3$BNR$_2$BH$_2$R$_2$N]$^-$ anion. Loss of an H$_2$ molecule causes release of the final cyclic dimer product and regeneration of the hydride complex. With respect to the mechanistic hypotheses formulated on the basis of experimental findings, our calculation show that pathway a is more favorable for all of the examined amine-boranes and especially for diisopropylamine–borane, due to the electron-donating nature of the iPr substituents. The complex with the [H$_3$BNR$_2$BH$_2$R$_2$N]$^-$ anion coordinated to the metal center is accessible for dimethylamine–borane and pyrrolidine–borane and inaccessible for the more sterically demanding diisopropylamine–borane, whereas the barrier to release of the cyclic dimer is very high in all cases. The possibility exists that the [Me$_2$N–BH$_2$]$_2$ and [(CH$_2$)$_4$N–BH$_2$]$_2$ cyclic dimers, which can be formed off-metal in solution, react with the Mg hydride to yield the complex containing the corresponding anion.

In spite of the analogies in catalytic activity for amine–borane dehydrocoupling between Mg- and Ca-based complexes, our theoretical analysis confirms the experimentally observed lower reactivity of Ca complexes. The dehydrogenation reaction involving the Ca-based complex can proceed only once a second amine–borane molecule coordinates to the metal center and intermolecular H$_2$ elimination occurs. Ca hydride formation is inaccessible, very likely because of the increase in cationic radius. The distance between the Ca center and the BH hydride is too long to allow transfer to the metal center. The results reported herein are of particular interest be-

↖↖ **These are not the final page numbers!**

cause, although amine–borane dehydrogenation is now well-established, mechanistic insight is still lacking for many systems. Future work will continue the theoretical exploration and rationalization of the catalytic behavior toward dehydrogenation/dehydrocoupling of amine–boranes of a more extended range of group 2 metals and d^0 species of the early transition metals.

Experimental Section

Geometry optimizations and frequency calculations for all reactants, intermediates, products, and transition states were performed at the DFT level of theory by using the B3PW91 functional[17] as implemented in the Gaussian 03[18] code. For all the atoms, including Mg and Ca, all-electron standard 6-311G** basis sets of Pople and co-workers were employed. For each optimized stationary point vibrational analysis was performed to establish its nature as a minimum or saddle point, and zero-point vibrational energy (ZPVE) corrections were included in all relative energies (ΔE). For transition states it was carefully checked that the vibrational mode associated with the imaginary frequency corresponded to the correct movement of the involved atoms. Furthermore, the intrinsic reaction coordinate (IRC)[19] method was used to check that the localized TSs correctly connect to the corresponding minima along the imaginary mode of vibration. The free energies G were calculated for $T = 298.15$ K. All relative energies are reported in kilocalories per mole. Implicit solvent effects were calculated through the conductor-like polarizable continuum model (CPCM).[20] Since preliminary calculations clearly showed that geometry relaxation effects were not significant, single-point calculations were performed by using more extended 6-311+G** basis sets on the fully optimized geometry of each stationary point along the reaction paths. Calculations were carried out in THF solvent ($\varepsilon = 7.6$). Reaction Gibbs free energies in solution ΔG_{sol} were calculated for each process as the sum of two contributions: a gas-phase reaction free energy ΔG_{gas} and a solvation reaction free energy ΔG_{solv} calculated with the continuum approach. NBO charge analysis[21] was carried out on the structures of some intercepted stationary points.

[1] S. G. Shore, R. W. Parry, *J. Am. Chem. Soc.* **1955**, *77*, 6084–6085.
[2] A. B. Burg, H. I. Schlesinger, *J. Am. Chem. Soc.* **1937**, *59*, 780–787.
[3] A. Stock, E. Pohland, *Ber. Dtsch. Chem. Ges.* **1925**, *58*, 657.
[4] R. D. Schultz, R. W. Parry, *J. Am. Chem. Soc.* **1958**, *80*, 4–8.
[5] S. G. Shore, P. R. Girardot, R. W. Parry, *J. Am. Chem. Soc.* **1958**, *80*, 20–24.
[6] R. W. Parry, *J. Chem. Educ.* **1997**, *74*, 512.
[7] U.S. DOE. Basic Research Needs for the Hydrogen Economy (http://www.sc.doe.gov/bes/reports/files/NHE_rpt.pdf).
[8] a) D. A. Dixon, M. Gutowski, *J. Phys. Chem. A* **2005**, *109*, 5129; b) A. Staubitz, M. Besora, J. N. Harvey, I. Manners, *Inorg. Chem.* **2008**, *47*, 5910–5918.
[9] Selection of papers reporting the use of transition metals for the H_3NBH_3 and amine-borane derivatives dehydrocoupling: a) C. A. Jaska, K. Temple, A. J. Lough, I. Manners, *Chem. Commun.* **2001**, 962–963; b) M. C. Denney, V. Pons, D. M. Heinekey, K. I. Goldberg, *J. Am. Chem. Soc.* **2006**, *128*, 12048–12049; c) R. J. Keaton, J. M. Blacquiere, R. T. Baker, *J. Am. Chem. Soc.* **2007**, *129*, 1844–1845; d) B. L. Dietrich, K. I. Goldberg, D. M. Heinekey, T. Autrey, J. C. Linehan, *Inorg. Chem.* **2008**, *47*, 8583–8585; e) T. M. Douglas, A. M. Chaplin, A. S. Weller, *J. Am. Chem. Soc.* **2008**, *130*, 14432–14433; f) N. Blaquiere, S. Diallo-Garcia, S. I. Gorelsky, D. A. Black, K. Fagnou, *J. Am. Chem. Soc.* **2008**, *130*, 14034–14035; g) M. Käß, A. Friedrich, M. Drees, S. Schneider, *Angew. Chem.* **2009**, *121*, 922–924; *Angew. Chem. Int. Ed.* **2009**, *48*, 905–907; h) A. Friedrich, M. Drees, S. Schneider, *Chem. Eur. J.* **2009**, *15*, 10339–10342; i) T. M. Douglas, A. M. Chaplin, A. S. Weller, X. Yang, M. B. Hall, *J. Am. Chem. Soc.* **2009**, *131*, 15440–15456; j) Y. Jiang, H. Berke, *Chem. Commun.* **2007**, 3571–3573; k) A. B. Chaplin, A. S. Weller, *Inorg. Chem.* **2010**, *49*, 1111–1115; l) R. T. Baker, J. C. Gordon, C. W. Hamilton, N. J. Henson, P.-H. Lin, S. Maguire, M. Murugesu, B. L. Scott, N. C. Smythe, *J. Am. Chem. Soc.* **2012**, *134*, 5598–5609.
[10] a) A. Staubitz, A. P. M. Robertson, M. E. Sloan, I. Manners, *Chem. Rev.* **2010**, *110*, 4023–4078; b) A. Staubitz, A. P. M. Robertson, I. Manners, *Chem. Rev.* **2010**, *110*, 4079–4124.
[11] V. Butera, N. Russo, E. Sicilia, *Chem. Eur. J.* **2011**, *17*, 14586–14592.
[12] a) M. R. Crimmin, A. G. M. Barrett, M. S. Hill, P. B. Hitchcock, P. A. Procopiou, *Inorg. Chem.* **2007**, *46*, 10410–10415; b) D. J. Liptrot, M. S. Hill, M. F. Mahon, D. J. MacDougall, *Chem. Eur. J.* **2010**, *16*, 8508–8515; c) M. S. Hill, M. Hodgson, D. J. Liprot, M. F. Mahon, *Dalton Trans.* **2011**, *40*, 7783–7790; d) P. Bellham, M. S. Hill, D. J. Liptrot, D. J. MacDougall, M. F. Mahon, *Chem. Commun.* **2011**, *47*, 9060–9062; e) P. Bellham,, M. S. Hill, G. Kociok-Kohn, D. J. Liptrot, *Dalton Trans.* **2013**, *42*, 737–745; f) J. Spielmann, G. Jansen, H. Bandmann, S. Harder, *Angew. Chem.* **2008**, *120*, 6386; *Angew. Chem. Int. Ed.* **2008**, *47*, 6290; g) J. Spielmann, S. Harder, *J. Am. Chem. Soc.* **2009**, *131*, 5064; h) J. Spielmann, M. Bolte, S. Harder, *Chem. Commun.* **2009**, 6934; i) J. Spielmann, D. F.-J. Piesik, S. Harder, *Chem. Eur. J.* **2010**, *16*, 8307–8318; j) H. J. Cowley, M. S. Holt, R. L. Melen, J. M. Rawson, D. S. Wright, *Chem. Commun.* **2011**, *47*, 2682; k) M. M. Hansmann, R. L. Melen, D. S. Wright, *Chem. Sci.* **2011**, *2*, 1554; l) R. J. Less, R. L. Melen, D. S. Wright, *RSC Adv.* **2012**, *2*, 2191.
[13] a) G. Pawelke, H. Bürger, *Appl. Organomet. Chem.* **1996**, *10*, 147; b) D. J. Brauer, H. Bürger, T. Dittmar, G. J. Pawelke, *J. Organomet. Chem.* **1995**, *493*, 167; c) D. J. Brauer, S. Buchheim-Spiegel, H. Bürger, R. Gielen, G. Pawelke, J. Rothe, *Organometallics* **1997**, *16*, 5321; d) B. C. Dutmer, T. M. Gilbert, *Organometallics* **2011**, *30*, 778.
[14] C. J. Stevens, R. Dallanegra, A. B. Chaplin, A. S. Weller, S. A. Macgregor, B. Ward, D. McKay, G. Alcaraz, S. Sabo-Etienne, *Chem. Eur. J.* **2011**, *17*, 3011–3020.
[15] a) L. Euzenat, D. Horhant, Y. Ribourdouille, C. Duriez, G. Alcaraz, M. Vaultier, *Chem. Commun.* **2003**, 2280; b) C. Y. Tang, A. L. Thompson, S. Aldridge, *Angew. Chem.* **2010**, *122*, 933–937; *Angew. Chem. Int. Ed.* **2010**, *49*, 921–925.
[16] M. Arrowsmith, M. R. Crimmin, A. G. M. Barrett, M. S. Hill, G. Kaciock-Köhn, P. A. Procopiou, *Organometallics* **2011**, *30*, 1493–1506.
[17] a) A. D. Becke, *J. Chem. Phys.* **1993**, *98*, 5648–5652; b) J. P. Perdew, Y. Wang, *Phys. Rev. B* **1992**, *45*, 13244–13249.
[18] Gaussian 03, Revision C.02, M. J. Frisch, G. W. Trucks, H. B. Schlegel, G. E. Scuseria, M. A. Robb, J. R. Cheeseman, J. A. Montgomery, Jr., T. Vreven, K. N. Kudin, J. C. Burant, J. M. Millam, S. S. Iyengar, J. Tomasi, V. Barone, B. Mennucci, M. Cossi, G. Scalmani, N. Rega, G. A. Petersson, H. Nakatsuji, M. Hada, M. Ehara, K. Toyota, R. Fukuda, J. Hasegawa, M. Ishida, T. Nakajima, Y. Honda, O. Kitao, H. Nakai, M. Klene, X. Li, J. E. Knox, H. P. Hratchian, J. B. Cross, V. Bakken, C. Adamo, J. Jaramillo, R. Gomperts, R. E. Stratmann, O. Yazyev, A. J. Austin, R. Cammi, C. Pomelli, J. W. Ochterski, P. Y. Ayala, K. Morokuma, G. A. Voth, P. Salvador, J. J. Dannenberg, V. G. Zakrzewski, S. Dapprich, A. D. Daniels, M. C. Strain, O. Farkas, D. K. Malick, A. D. Rabuck, K. Raghavachari, J. B. Foresman, J. V. Ortiz, Q. Cui, A. G. Baboul, S. Clifford, J. Cioslowski, B. B. Stefanov, G. Liu, A. Liashenko, P. Piskorz, I. Komaromi, R. L. Martin, D. J. Fox, T. Keith, M. A. Al-Laham, C. Y. Peng, A. Nanayakkara, M. Challacombe, P. M. W. Gill, B. Johnson, W. Chen, M. W. Wong, C. Gonzalez, J. A. Pople, Gaussian, Inc., Wallingford CT, 2004.

[19] a) K. Fukui, *J. Phys. Chem.* **1970**, *74*, 4161–4163; b) C. Gonzalez, H. B. Schlegel, *J. Chem. Phys.* **1989**, *90*, 2154–2161.

[20] a) V. Barone, M. Cossi, *J. Phys. Chem. A* **1998**, *102*, 1995–2001; b) M. Cossi, N. Rega, G. Scalmani, V. Barone, *J. Comput. Chem.* **2003**, *24*, 669–681.

[21] a) J. E. Carpenter, F. Weinhold, *J. Mol. Struct.* **1988**, *169*, 41; b) J. E. Carpenter, F. Weinhold, *The Structure of Small Molecules and Ions*, Plenum, New York, **1988**.
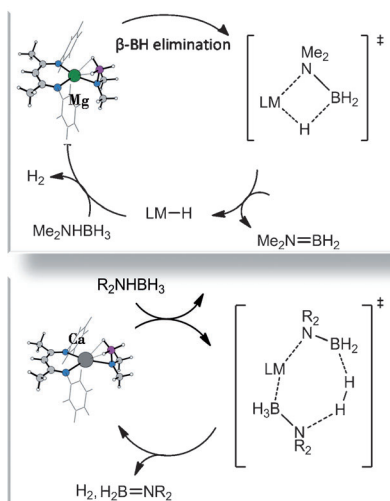
↖↖ These are not the final page numbers!

Dehydrocoupling of amine–boranes assisted by Mg- and Ca-based complexes was studied by DFT calculations to assess the viability of the pathways of the mechanistic scheme proposed on the basis of experimental evidence and to determine whether different ionic radii and charge densities are responsible for the observed differences in reactivity of Mg and Ca complexes (see scheme). The influence of the steric demand of amine–boranes on the course of the reaction was examined by performing calculations on the dehydrogenation of dimethylamine–borane, pyrrolidine–borane, and diisopropylamine–borane.

These are not the final page numbers! ↗↗